Published in final edited form as:
J Surg Oncol. 2011 September 1; 104(3): 323–332. doi:10.1002/jso.21943.

The clinical use of indocyanine green as a near-infrared fluorescent contrast agent for image-guided oncologic surgery

Boudewijn E. Schaafsma, MD[1], **J.Sven D. Mieog, MD**[1], **Merlijn Hutteman, MSc**[1], **Joost R. van der Vorst, MD**[1], **Peter J.K. Kuppen, PhD**[1], **Clemens W.G.M. Löwik, PhD**[2], **John V. Frangioni, MD, PhD**[3,4], **Cornelis J.H. van de Velde, MD, PhD**[1], and **Alexander L. Vahrmeijer, MD, PhD**[1,*]

[1]Department of Surgery, Leiden University Medical Center, Leiden, The Netherlands [2]Department of Endocrinology, Leiden University Medical Center, Leiden, The Netherlands [3]Division of Hematology/Oncology, Department of Medicine, Beth Israel Deaconess Medical Center, Boston, MA [4]Department of Radiology, Beth Israel Deaconess Medical Center, Boston, MA

Abstract

Optical imaging using near-infrared (NIR) fluorescence provides new prospects for general and oncologic surgery. ICG is currently utilised in NIR fluorescence cancer-related surgery for three indications: sentinel lymph node (SLN) mapping, intraoperative identification of solid tumours, and angiography during reconstructive surgery. Therefore, understanding its advantages and limitations is of significant importance. Although non-targeted and non-conjugatable, ICG appears to be laying the foundation for more widespread use of NIR fluorescence-guided surgery.

Keywords

optical imaging; fluorescence; sentinel lymph node; angiography; tumour detection

INTRODUCTION

The identification of structures that need to be resected (e.g. tumour tissue, lymph nodes) and structures that need to be spared (e.g. nerves, ureters, bile ducts) is of paramount importance in oncologic surgery. In daily surgical practice, surgeons mainly rely on palpation and visual inspection. However, tumour-positive resection margins and surgical morbidity as a result of damage to vital structures are not uncommon. Thus, there is a need for new intraoperative imaging modalities that can provide real-time assessment of tumour borders and affected lymph nodes, while eliminating the risk of damage to vital structures.

Optical imaging using near-infrared (NIR) fluorescence is a new technique that can be used to visualise structures in real-time during surgery. Advantages of NIR fluorescent light (700–900 nm) include high tissue penetration (millimetres to centimetres deep) and low autofluorescence, thereby providing sufficient contrast [1]. Because the human eye is

*Corresponding author: Dr. Alexander L. Vahrmeijer, M.D., Ph.D. Albinusdreef 2, 2300 RC Leiden, The Netherlands Phone: +31715262309 Fax: +31715266750 a.l.vahrmeijer@lumc.nl.

CONFLICT OF INTEREST STATEMENT: John V. Frangioni: All FLARE technology is owned by Beth Israel Deaconess Medical Center, a teaching hospital of Harvard Medical School. As inventor, Dr. Frangioni may someday receive royalties if products are commercialized. Dr. Frangioni is the founder and unpaid director of The FLARE Foundation, a non-profit organization focused on promoting the dissemination of medical imaging technology for research and clinical use.

insensitive to NIR wavelengths, the use of NIR light does not alter the surgical field. Recently developed intraoperative imaging systems are able to provide simultaneous acquisition of surgical anatomy (white light, colour video) and NIR fluorescence signal [2–4]. Therefore, the use of NIR fluorescence imaging could potentially be of great value in the intraoperative detection of critical anatomical structures and oncologic targets.

In addition to NIR fluorescence imaging systems, exogenous NIR fluorescent contrast agents are necessary to visualise specific tissues. Ideally, tumour cells are labelled by targeted contrast agents. However, the only fluorescent contrast agents currently registered by the FDA and EMA for clinical applications are indocyanine green (ICG; peak emission ≈ 820 nm), methylene blue (peak emission ≈ 700 nm), and fluorescein (peak emission ≈ 520 nm, below NIR spectrum). This review is focused on the clinical use of ICG, due to its preferable fluorescent characteristics and widespread use in clinical research. ICG provides a higher signal-to-background ratio because of lower autofluorescence and increased tissue penetration at 820 nm compared to lower wavelengths and has a greater “brightness” (i.e., quantum yield) compared to methylene blue [5].

ICG is currently utilised in NIR fluorescence image-guided oncologic surgery for multiple indications. NIR fluorescence imaging has the potential to improve sentinel lymph node (SLN) mapping in multiple types of cancer, by real-time transcutaneous and intraoperative visualisation of lymphatic channels and subsequent detection of the SLN [3,4,6–29]. Additionally, ICG NIR fluorescence is used for endoscopic marking of colorectal tumours and intraoperative identification of certain solid tumours after intravenous injection [30–32]. Moreover, NIR fluorescence angiography using ICG can be used in intraoperative assessment of tissue perfusion in reconstructive surgery for ablative defects following oncologic surgery [33].

The aim of this paper is to review the available clinical studies using ICG in NIR fluorescence-guided cancer surgery in order to understand current applications, limitations, and future prospects.

NIR FLUORESCENCE IMAGING

Clinically available NIR imaging systems

Several NIR fluorescence imaging systems have been described for intraoperative clinical use (reviewed in Gioux et al. [34]). Although differing in their technical specifications, all of these systems provide the surgeon with an image of the NIR fluorescence signal that would otherwise be invisible to the human eye (Table I). The majority of clinical studies published to date use the commercially available Photodynamic Eye (PDE, Hamamatsu Photonics, Hamamatsu, Japan) imaging camera system [18]. Other commercially available systems are the SPY system (Novadaq Technologies, Concord, ON, Canada) and the Fluobeam (Fluoptics, Grenoble, France). Several others imaging systems have been used in clinical studies but are not commercially available: HyperEye [2] (Kochi Medical School, Kochi, Japan), the FLARE and Mini-FLARE [3] (Beth Israel Deaconess Hospital, Boston, MA, USA), the FDPM imager [35] (Texas Medical Center, Houston, TX, USA), and a prototype camera system from Munich [4] (Technical University Munich, Munich, Germany and SurgOptix Inc., Redwood Shores, CA, USA) .

Indocyanine green

ICG is a negatively charged, amphiphilic, water-soluble but relatively hydrophobic, tricarbocyanine with a molecular mass of 776 Da [36,37]. ICG has been registered for several decades to determine cardiac output, hepatic function, and ophthalmic perfusion. Rapid registration was attributable to favourable characteristics such as the confinement to

the vascular compartment by binding to plasma proteins, the fast and almost exclusive excretion into the bile, and the very low toxicity of ICG [38,39]. ICG is safe to use, as the number of allergic reactions is very low (1: 10 000, as reported by manufacturer). The dose used for standard diagnostic procedures lies between 0.1 and 0.5 mg/kg. Above 0.5 mg/kg, the incidence of immediate allergic reactions increases [40].

In plasma, ICG has an absorption peak around 807 nm and an emission peak around 822 nm, which is within the NIR window (Fig. 1). After intravenous administration, ICG has a short half-time of 150 to 180 seconds and is cleared exclusively by the liver [41]. Relatively hydrophobic ICG molecules bind rapidly and almost completely to serum proteins. Protein binding reduces aggregation, increases brightness (i.e., quantum yield) by over 3-fold, and increases effective hydrodynamic diameter to that of the bound proteins [38,42–44]. Hydrodynamic diameter has important implications for distribution and transport of ICG for tumour visualisation and retention in the SLN as discussed below [6,45,46].

SENTINEL LYMPH NODE MAPPING

NIR fluorescence imaging provides new opportunities to improve and extend the indications of the SLN procedure. Gamma ray-emitting radiotracers and blue dyes are currently used as the standard of care in clinical practice. However, the use of gamma ray-emitting radiotracers requires involvement of a nuclear medicine physician, and localisation of the SLN can be difficult using a handheld gamma probe. Also, preoperative access to the injection site is required. Blue dyes cannot be easily seen through the skin and fatty tissue. Additionally, the learning curve for the standard SLN procedure using these techniques is estimated to be 60 required cases for technical proficiency when working with breast cancer patients [47].

NIR fluorescence imaging using ICG has been shown to visualise superficial lymphatic channels transcutaneously [14]. Thereby, it could potentially reduce time of surgery and improve localisation of the SLN so that a small incision can be made, while maintaining a high identification rate. Moreover, the NIR fluorescence signal could aid the pathologist in both preparing and analysing the tissue specimen [13,18]. It should be noted, however, that NIR fluorescence detection is in the millimetre to centimetre range, far less than radioactive tracers, which requires caution when examining thick tissues.

Studies using ICG as a NIR fluorescent lymphatic tracer in SLN procedures are summarized in Table II. A total of 25 studies have been published using ICG as lymphatic tracer in SLN procedures in breast, skin, gastrointestinal, non-small cell lung, oropharyngeal and gynaecological cancer [3,4,7–29]. Differences in imaging systems, ICG doses and injection sites prevent direct comparison of the results. In the next sections, the results will be discussed for each tumour type separately.

Breast cancer

Eleven studies report the use of ICG as a NIR fluorescent lymphatic tracer in the SLN procedure in a total of 548 breast cancer patients [3,12–21]. Before the introduction of NIR fluorescence imaging systems, Motomura et al.[48] used only the intrinsic green colour of ICG and identified the SLN in 73.8% of patients. After the introduction of intraoperative NIR fluorescence imaging systems, higher identification rates of 87.5% to 100% (aggregate 98.6%) were obtained and an average of 3.4 (range 1.5 to 5.4) SLNs were identified. Two studies performed an axillary dissection irrespective of the SLN status and found an aggregate false-negative rate of 7.7% in 39 patients with a negative SLN [12,14]. Additionally, as a result of the capability of NIR fluorescence light to penetrate tissue, ICG offers non-invasive imaging of lymphatic flow (Fig. 2). Upon injection of ICG, travel time

to the axilla is 1 to 10 min [13,16]. The small size of the ICG particle is probably responsible for this relatively high velocity, which has logistical advantages compared to relatively larger gamma ray-emitting radiotracers. Hojo et al. [15] compared ICG to patent blue in 113 patients and showed that ICG had a higher identification rate (100%) than patent blue (93%). Three studies compared the method of SLN detection by ICG fluorescence (71 out of 73 nodes) and the radiotracer (70 out of 73 nodes) [12,15,17]. Both techniques are used simultaneously in all studies; therefore, both identification rates were similar. However, no comparison can be made as to whether one is superior to the other.

Several factors influence the success of the SLN procedure using ICG. In the reported clinical trials, various doses of ICG have been used ranging from 0.01 mM to 6.4 mM. Sevick-Muraca et al. [16] found that a minimal dose of 0.01 mM ICG is required for successful SLN mapping. Mieog et al. [17] allocated patients in groups of escalating ICG concentrations from 0.05 mM to 1.0 mM diluted in albumin and obtained the highest brightness of the SLN using a concentration between 0.4 mM to 0.8 mM ICG (1.6 ml injection volume). Additionally, because of its relatively small hydrodynamic diameter, ICG is able to pass through the sentinel node to second-tier nodes and eventually spread through the subcutaneous tissue [18]. To surpass this effect, imaging should to be performed shortly after ICG administration. Furthermore, as a result of the limited tissue penetration of the fluorescent signal, visualisation is limited once ICG has reached the axillary fossa, particularly in patients with a high body mass index [13,19,49].

Skin cancer

Four studies reported the use of ICG as an NIR fluorescent lymphatic tracer in the SLN procedure in a total of 42 skin cancer patients [22–25]. The NIR fluorescence-guided SLN procedure resulted in identification of at least one SLN in 41 of the 42 patients (total number of SLNs identified was not reported). This is concordant with recent trials using conventional techniques, which showed a 93% to 100% identification rate [50,51]. Upon intradermal injection, ICG enables easy visualisation of the subcutaneous lymphatic drainage, which takes approximately 15 min after injection to reach the SLN and stays visible for at least three hours [22]. The results of these studies are promising. However, larger trials are needed to assess patient benefit.

Gastro-intestinal cancer

Nodal status is one of the most important prognostic factors in gastric and colorectal cancer. It is hypothesised that the SLN procedure in gastro-intestinal cancer patients can improve nodal staging [52]. Currently, prophylactic lymphadenectomy is considered the standard of care for these patients. Several studies have assessed the use of the SLN procedure using radiotracers or blue dye, or both [52–54]. However, these studies show varying lymphatic drainage patterns and report high rates of skip metastases, preventing the introduction of the SLN procedure in general clinical practice.

In early gastric cancer, four studies reported the use of ICG as NIR fluorescent lymphatic tracer in the SLN procedure in a total of 158 patients [26–29]. ICG was injected during surgery or at one to three days before surgery. After both preoperative subserosal and preoperative submucosal injection of ICG, lymphatic vessels draining the tumour could be visualised [26–29]. The identification rates ranged from 90.9% to 96.4% (aggregate 94.9%) with an average number of SLNs identified of 3.0 to 7.5 [26–29]. The false-negative rates reported in these studies ranged from 14.3% to 33.3% in T1 tumours, which increased with tumour stage up to 75% in T3 gastric tumours [26,28,29]. However, the number of patients in these tumour stages with tumour-positive lymph nodes is small (range 3–10).

Several factors influence the success of SLN procedure in gastric cancer. Frequent leakage was observed from lacerated lymphatic vessels during the SLN mapping in patients with intraoperative ICG injection [28]. Preoperative endoscopic ICG injection results in a higher number of fluorescent lymph nodes and lower false negative rate compared to intraoperative injection [28]. Due to the longer interval between injection and imaging, it is expected that ICG passes through the SLN to the higher-tier nodes. In addition to fluorescence imaging, ICG absorption imaging has been used for SLN detection in early gastric cancer during endoscopy [27,54–57] However, as shown by Miyashiro et al. [27], fluorescence provides much higher contrast than absorption and is therefore preferred.

In colorectal cancer, two studies reported the use of ICG as an NIR fluorescent lymphatic tracer in a total of 51 patients with an identification rate of 88.5% and 92%, respectively, and an average number of identified SLNs of 2.1 and 2.6, respectively [7,26]. The false negative rate was 4 out of 9 (44%) patients with tumour-positive lymph nodes.

When the SLN procedure is used for nodal staging to determine prognosis and possible adjuvant therapy, as has been suggested for colorectal cancer, an *ex vivo* approach can be considered [58]. Using an *ex vivo* approach, more optimised NIR fluorescent dyes can be used, which are not yet approved for *in vivo* administration, such as IRDye 800CW (LI-COR, Lincoln, NE, USA). Such dyes can also be conjugated covalently to albumin or nanocolloid to increase lymph node retention [42,59]. This *ex vivo* strategy was successfully applied in a recent clinical study [60].

Conclusions for sentinel lymph node mapping

NIR fluorescence SLN mapping has shown excellent results to date in breast and skin cancer. Therefore, the use of ICG should be particularly attractive to hospitals unable to work with radioactive isotopes as an adjunct or possible replacement to the use of blue dye alone [15,17]. Direct comparison between ICG fluorescence and radiotracers in adequately powered clinical trials, however, has not yet been performed. In gastrointestinal cancer, SLN procedures using ICG obtain high identification rates, although the high false negative rates in the small patient samples require further assessment. Additionally, the feasibility of NIR fluorescence SLN mapping using ICG has also been assessed in single studies in cervical, vulvar, anal, oropharyngeal and non-small cell lung cancer [4,8–11].

As the available data on ICG fluorescence in the sentinel lymph node procedure is relatively limited, conclusion on direct patient benefit and clinical outcome can not yet be drawn. Currently, several groups are performing clinical trials using NIR fluorescence imaging and ICG in the SLN procedure in multiple malignancies (JPRN-UMIN000003035, NCT00264602, NTR1981, NTR1983, NTR2003, NTR2084, NTR2479, NTR2480, NTR2481, NTR2482, as retrieved from http://apps.who.int/trialsearch/ on Jan 3, 2011).

TUMOUR IMAGING

The main goal of cancer surgery is the complete and “en-bloc” excision of tumours with adequate tumour-free margins while minimising surgical morbidity. Presently, though, intraoperative assessment of tumour margins relies on palpation and visual inspection. NIR fluorescence imaging is a promising technique for intraoperative tumour identification. NIR fluorescent probes that specifically target tumour cells could aid the surgeon in determining resection margins and possibly reduce the risk of locoregional recurrence [61,62]. Although ICG is a non-targeted probe, it can provide NIR fluorescence tumour localisation in a limited number of hepatobiliary cancer patients [31,63–66], either due to physiological uptake in well-differentiated tumours or rim uptake as a result of leakage and retention in poorly-differentiated tumours and colorectal metastases [32,67].

Imaging of hepatobiliary cancer

Liver resection is the only curative option in the treatment of hepatobiliary cancer. Intrahepatic recurrence rates after resection of colorectal cancer metastases range from 11% to 37.5% and the majority of these recurrences appear within two years after resection [68–72]. A possible explanation for this high intrahepatic recurrence rate is that these hepatic metastases were present at time of resection of the liver metastases but were undetected by preoperative imaging and intraoperative ultrasound. NIR fluorescence detection is a new technique to intraoperatively visualise hepatobiliary cancer.

ICG is excreted exclusively into the bile, which allows real-time NIR fluorescence cholangiography of biliary anatomy during cholecystectomy and other hepatobiliary surgery [73–75]. This technique provides a reliable roadmap of the biliary tree, which enables the surgeon to avoid injuring the bile duct [73]. In hepatobiliary cancer, it is hypothesised that the NIR fluorescent signal in or around the tumour is caused by passive accumulation due to hampered biliary excretion, which, in the case of a colorectal liver metastasis, results in a fluorescent rim around the tumour (Fig. 3) [31]. To date, five Japanese studies have reported the use of ICG in NIR fluorescence imaging of hepatobiliary cancer including colorectal metastasis, hepatocellular carcinoma and cholangiocarcinoma [31,63–66]. To identify liver tumours, the best time window is beyond 24 hours after injection, when most ICG is washed out of the healthy liver parenchyma and is still present in and around the tumour tissue [31].

In patients with hepatocellular carcinoma or colorectal liver metastases, 98.1% to 100% of the lesions were detected using NIR fluorescence in the resection tissue specimen [31,64,66]. However, due to limited penetration of the NIR fluorescent signal, intraoperative detection of deeper located tumours was not possible (Ishizawa et al. [31] reported a maximal detection depth of 8 mm). Tumours located at the liver surface provide a bright fluorescent signal and are easily detected, which is especially useful for colorectal liver metastases as these are mostly located on the surface of the liver parenchyma. In these studies this resulted in detection of new small superficial lesions by NIR fluorescence imaging that could not be detected by intraoperative ultrasonography or by visual inspection [31,66].

In the case of cholangiocarcinoma, Harada et al. [65] showed ICG fluorescence on the liver surface in the regions of liver with cholestasis caused by bile duct tumour invasion or thrombi. Although the tumour itself was not fluorescent, the information provided by NIR fluorescence imaging can help to estimate the extent of the bile duct tumour infiltration.

In conclusion, ICG fluorescence might be of value during hepatobiliary surgery when used as an adjunct to intraoperative ultrasound, and could be particularly useful in the intraoperative identification of small superficially located liver tumours. However, to identify deeper tumours, intraoperative ultrasound imaging is still required. Additionally, ICG fluorescence can aid in the identification of tumour lesions during pathological examination.

Marking tumours

Endoscopic marking of intestinal lesions is essential in laparoscopic surgery or when difficulty in locating the lesion during resection is anticipated [30,67]. India ink is a frequently used dye, but is associated with complications and side effects and alters the surgical field [67]. ICG could be a more suitable dye for tattooing, because of fewer side effects, relatively long absorption time (up to 14 days), and potential increased detection using NIR fluorescence compared to macroscopic colour perception [30,76,77].

Watanabe et al. [30] showed accurate and clear NIR fluorescence tumour localization after preoperative peritumoral injection of ICG. In all 10 patients, the NIR fluorescence signal was detected in the colon tumour and could be visualised clearly for at least 72 to 120 hours, whereas the marked location detection based on the intrinsic green colour of ICG was possible in only 2 patients.

Other solid tumours

It has been proposed that ICG can be used in intraoperative imaging of solid tumours other than hepatobiliary cancer. The enhanced permeability and retention (EPR) effect can potentially be used for tumour imaging. Due to newly formed, more porous blood vessels, molecules can passively accumulate in tumour tissue. Furthermore, a poorly developed tumoral lymphatic system results in increased retention [78–81].

Exploiting the EPR effect, 6 clinical studies with breast tumours used ICG for tumour identification in an outpatient, mammography-like setting [32,81–85]. These studies used optical tomography, which has higher depth penetration and potentially higher specificity, albeit with much lower resolution. During the first 10 min, ICG was retained in the breast tumour tissue and provided contrast to the surrounding healthy tissue [81,82]. Hagen et al. [32] and Poellinger et al. [85] used a prototype fluorescence mammographic imaging system and showed the ability to discriminate between malignant and benign lesions after intravenous administration of ICG. However, in an intraoperative setting a higher tumour-to-background ratio would be needed to provide sufficient tumour demarcation.

Additionally, ICG can be useful as a diagnostic tool to estimate the invasiveness of early gastric cancer during endoscopy. Four Japanese studies used NIR fluorescence endoscopy using ICG as contrast agent to differentiate between mucosal and submucosal or more invasive tumours, and obtained a diagnostic accuracy of 85% up to 93% [86–89]. The NIR fluorescence signal was visible up to 3 min in tumour tissue compared to several seconds in healthy tissue [86]. Therefore, ICG might be useful to distinguish mucosal cancer from submucosal and deeper cancers, which is a risk factor for lymph node metastasis. However, the short duration of the signal limits its use in a surgical setting.

In conclusion, the lack of direct tumour targeting properties prevents the introduction of ICG as NIR fluorescent probe in most tumour types in an intraoperative setting.

ANGIOGRAPHY IN RECONSTRUCTIVE SURGERY

Due to its biological characteristics following intravenous injection, ICG is a suitable contrast agent for NIR fluorescence angiography. ICG is mainly bound to plasma proteins and therefore remains predominantly in the intravascular space. Additionally, because of its rapid washout, ICG permits consecutive measurements. ICG angiography has been used in the evaluation of coronary artery bypass grafts, peripheral vascular disease, and solid organ transplantation [2,90–94].

In reconstructive surgery, intraoperative evaluation of skin flap viability is highly desirable, as loss of skin flaps is catastrophic and may produce even larger tissue deficits. Commonly used subjective methods such as tissue colour, capillary refill, dermal bleeding and more objective methods such as skin temperature, fluorescein dye perfusion, transcutaneous oxygen monitoring and Doppler ultrasound, are not optimal. NIR fluorescence angiography using ICG allows the surgeon to visualize arterial inflow, venous return and tissue perfusion, prior to harvest and after flap transfer. To date, several studies of NIR fluorescence angiography using ICG in reconstructive surgery after oncologic surgery have been performed [33,95–102].

As a result of great variation in perforating vessels and their perfusion zones, it can be challenging to select the optimal vessel to transfer a flap. NIR fluorescence angiography using ICG is able to successfully identify perfusion zones intraoperatively in various types of flaps, including transverse rectus abdominis musculocutaneous flaps, deep inferior epigastric perforator flaps and superficial inferior epigastric artery flaps (Fig. 4) [96–98,102]. In these studies, areas with fluorescence filling defects correlated with poor clinical outcome [97,101,102]. Therefore, intraoperative measurements of the flap perfusion allows intraoperative surgical decision making based on accurate assessment of flap vascularity.

Additionally, after flap transfer, NIR fluorescence angiography can detect impaired flap blood flow and can be helpful for differentiating among poor arterial inflow, poor venous outflow, or poor perfusion [100,101]. Rapid identification of vascular compromise allows direct intervention and increased flap salvage. Komorowska-Timek et al. [101] reported that using ICG NIR fluorescence angiography resulted in a favourable postoperative complication rate after breast reconstruction compared to a historic cohort (4% vs. 15.1%). Furthermore, in flap re-exploration, NIR fluorescence angiography using ICG can provide excellent diagnostic accuracy for detecting microvascular thrombosis [103]. Therefore, intraoperative assessment using ICG in NIR fluorescence angiography may be of great value in reconstructive surgery.

DISCUSSION AND FUTURE PERSPECTIVES

The recent introduction of NIR fluorescence image guidance provides new opportunities for surgery, particularly cancer surgery. Currently, ICG and methylene blue are the only clinically available NIR fluorescent probes and the reported clinical experience to date focuses on ICG. Clinical experience with ICG for intraoperative NIR fluorescence imaging is rather extensive and shows a favourable safety profile.

The current use of ICG in tumour detection and demarcation is limited because ICG cannot be conjugated to tumour specific targets, which makes ICG a non-targeted probe. Because ICG is not an ideal fluorescent probe, multiple novel fluorophores with improved optical properties, such as IRDye 800CW, have been developed. Moreover, these novel fluorophores can be conjugated to specific ligands. Various mechanisms are available to target tumour cells, for example tumour specific cell surface markers, enzymatic activity or increased glucose metabolism (reviewed in Keereweer et al. [104]). Multiple targeted probes are commercially available and have successfully been tested in animal studies [61,105–109]. Translating these preclinical results to clinical trials remains a major challenge. Several academic and industry groups have communicated the intention to move novel probes, such as IRDye 800CW, to the clinic and the first toxicity results for this purpose have been published [110].

Moreover, development of new imaging systems will further improve NIR fluorescence image-guided surgery. NIR fluorescence laparoscopic imaging systems are currently being developed, and a commercial system from Olympus is already being marketed, which will allow NIR fluorescence guided-surgery in a minimally invasive setting.[5,73,74,111] Various techniques are being evaluated to correct photon scattering and thereby enhance the depth at which NIR fluorescent signal can be detected [112–114].

When these improved NIR fluorescence imaging systems and probes become clinically available, indications for NIR fluorescence image-guided cancer surgery will be greatly expanded.

In conclusion, the availability of ICG permitted rapid clinical translation of NIR fluorescence intraoperative imaging to cancer surgery. ICG presents a new, safe and

sensitive alternative or addition to the conventional SLN procedure; although, conclusions on direct patient benefit and clinical outcome cannot yet be drawn. Moreover, the use of ICG allows objective assessment of flap perfusion in reconstructive surgery and provides opportunities for intraoperative tumour imaging.

List of Abbreviations

ICG	indocyanine green
NIR	near-infrared
SLN	sentinel lymph node

Acknowledgments

We thank Lindsey Gendall for editing.

Sources of Financial Support: This work was supported in part by NIH grant R01-CA-115296 and R01-EB-005805 and the Dutch Cancer Society grant UL2010-4732. J.S.D. Mieog is a MD-medical research trainee funded by The Netherlands Organisation for Health Research and Development (grant 92003526).

REFERENCES

1. Frangioni JV. New technologies for human cancer imaging. J Clin Oncol. 2008; 26:4012–4021. [PubMed: 18711192]
2. Handa T, Katare RG, Nishimori H, et al. New device for intraoperative graft assessment: HyperEye charge-coupled device camera system. Gen Thorac Cardiovasc Surg. 2010; 58:68–77. [PubMed: 20155342]
3. Troyan SL, Kianzad V, Gibbs-Strauss SL, et al. The FLARE Intraoperative Near-Infrared Fluorescence Imaging System: A First-in-Human Clinical Trial in Breast Cancer Sentinel Lymph Node Mapping. Ann Surg Oncol. 2009; 16:2943–2952. [PubMed: 19582506]
4. Crane LM, Themelis G, Pleijhuis RG, et al. Intraoperative Multispectral Fluorescence Imaging for the Detection of the Sentinel Lymph Node in Cervical Cancer: A Novel Concept. Mol Imaging Biol. 2010
5. Matsui A, Tanaka E, Choi HS, et al. Real-time intra-operative near-infrared fluorescence identification of the extrahepatic bile ducts using clinically available contrast agents. Surgery. 2010; 148:87–95. [PubMed: 20117813]
6. Tanaka E, Choi HS, Fujii H, et al. Image-guided oncologic surgery using invisible light: completed pre-clinical development for sentinel lymph node mapping. Ann Surg Oncol. 2006; 13:1671–1681. [PubMed: 17009138]
7. Noura S, Ohue M, Seki Y, et al. Feasibility of a lateral region sentinel node biopsy of lower rectal cancer guided by indocyanine green using a near-infrared camera system. Ann Surg Oncol. 2010; 17:144–151. [PubMed: 19774415]
8. Crane LM, Themelis G, Arts HJ, et al. Intraoperative near-infrared fluorescence imaging for sentinel lymph node detection in vulvar cancer: First clinical results. Gynecol Oncol. 2010
9. Bredell MG. Sentinel lymph node mapping by indocyanin green fluorescence imaging in oropharyngeal cancer - preliminary experience. Head Neck Oncol. 2010; 2:31. [PubMed: 21034503]
10. Yamashita SI, Tokuishi K, Anami K, et al. Video-assisted thoracoscopic indocyanine green fluorescence imaging system shows sentinel lymph nodes in non-small-cell lung cancer. J Thorac Cardiovasc Surg. 2010
11. Hirche C, Dresel S, Krempien R, et al. Sentinel node biopsy by indocyanine green retention fluorescence detection for inguinal lymph node staging of anal cancer: preliminary experience. Ann Surg Oncol. 2010; 17:2357–2362. [PubMed: 20217256]
12. Murawa D, Hirche C, Dresel S, et al. Sentinel lymph node biopsy in breast cancer guided by indocyanine green fluorescence. Br J Surg. 2009; 96:1289–1294. [PubMed: 19847873]

13. Kitai T, Inomoto T, Miwa M, et al. Fluorescence navigation with indocyanine green for detecting sentinel lymph nodes in breast cancer. Breast Cancer. 2005; 12:211–215. [PubMed: 16110291]
14. Hirche C, Murawa D, Mohr Z, et al. ICG fluorescence-guided sentinel node biopsy for axillary nodal staging in breast cancer. Breast Cancer Res Treat. 2010; 121:373–378. [PubMed: 20140704]
15. Hojo T, Nagao T, Kikuyama M, et al. Evaluation of sentinel node biopsy by combined fluorescent and dye method and lymph flow for breast cancer. Breast. 2010; 19:210–213. [PubMed: 20153649]
16. Sevick-Muraca EM, Sharma R, Rasmussen JC, et al. Imaging of lymph flow in breast cancer patients after microdose administration of a near-infrared fluorophore: feasibility study. Radiology. 2008; 246:734–741. [PubMed: 18223125]
17. Mieog JSD, Troyan SL, Hutteman M, et al. Towards Optimization of Imaging System and Lymphatic Tracer for Near-Infrared Fluorescent Sentinel Lymph Node Mapping in Breast Cancer. Ann Surg Oncol. 2011
18. Tagaya N, Yamazaki R, Nakagawa A, et al. Intraoperative identification of sentinel lymph nodes by near-infrared fluorescence imaging in patients with breast cancer. Am J Surg. 2008; 195:850–853. [PubMed: 18353274]
19. Ogasawara Y, Ikeda H, Takahashi M, et al. Evaluation of breast lymphatic pathways with indocyanine green fluorescence imaging in patients with breast cancer. World J Surg. 2008; 32:1924–1929. [PubMed: 18330628]
20. Tagaya N, Nakagawa A, Abe A, et al. Non-invasive identification of sentinel lymph node using indocyanine green fluorescence imaging in patient with breast cancer. The Open Surgical Oncology Journal. 2010; 2:71–74.
21. Tagaya N, Aoyagi H, Nakagawa A, et al. A novel approach for sentinel lymph node identification using fluorescence imaging and image overlay navigation surgery in patients with breast cancer. World J Surg. 2011; 35:154–158. [PubMed: 20931198]
22. Fujiwara M, Mizukami T, Suzuki A, et al. Sentinel lymph node detection in skin cancer patients using real-time fluorescence navigation with indocyanine green: preliminary experience. J Plast Reconstr Aesthet Surg. 2009; 62:e373–e378. [PubMed: 18556255]
23. Mizukami T, Fujiwara M, Suzuki A, et al. Sentinel lymph node detection by indocyanine green fluorescence imaging in skin cancer patients: technical refinement. The Open Surgical Oncology Journal. 2010; 2:57–61.
24. Tanaka R, Nakashima K, Fujimoto W. Sentinel lymph node detection in skin cancer using fluorescence navigation with indocyanine green. J Dermatol. 2009; 36:468–470. [PubMed: 19691754]
25. Tsujino Y, Mizumoto K, Matsuzaka Y, et al. Fluorescence navigation with indocyanine green for detecting sentinel nodes in extramammary Paget's disease and squamous cell carcinoma. J Dermatol. 2009; 36:90–94. [PubMed: 19284452]
26. Kusano M, Tajima Y, Yamazaki K, et al. Sentinel node mapping guided by indocyanine green fluorescence imaging: a new method for sentinel node navigation surgery in gastrointestinal cancer. Dig Surg. 2008; 25:103–108. [PubMed: 18379188]
27. Miyashiro I, Miyoshi N, Hiratsuka M, et al. Detection of sentinel node in gastric cancer surgery by indocyanine green fluorescence imaging: comparison with infrared imaging. Ann Surg Oncol. 2008; 15:1640–1643. [PubMed: 18379850]
28. Tajima Y, Yamazaki K, Masuda Y, et al. Sentinel node mapping guided by indocyanine green fluorescence imaging in gastric cancer. Ann Surg. 2009; 249:58–62. [PubMed: 19106676]
29. Tajima Y, Murakami M, Yamazaki K, et al. Sentinel node mapping guided by indocyanine green fluorescence imaging during laparoscopic surgery in gastric cancer. Ann Surg Oncol. 2010; 17:1787–1793. [PubMed: 20162462]
30. Watanabe M, Tsunoda A, Narita K, et al. Colonic tattooing using fluorescence imaging with light-emitting diode-activated indocyanine green: a feasibility study. Surg Today. 2009; 39:214–218. [PubMed: 19280280]
31. Ishizawa T, Fukushima N, Shibahara J, et al. Real-time identification of liver cancers by using indocyanine green fluorescent imaging. Cancer. 2009; 115:2491–2504. [PubMed: 19326450]

32. Hagen A, Grosenick D, Macdonald R, et al. Late-fluorescence mammography assesses tumor capillary permeability and differentiates malignant from benign lesions. Opt Express. 2009; 17:17016–17033. [PubMed: 19770920]
33. Lee BT, Matsui A, Hutteman M, et al. Intraoperative near-infrared fluorescence imaging in perforator flap reconstruction: current research and early clinical experience. J Reconstr Microsurg. 2010; 26:59–65. [PubMed: 20027541]
34. Gioux S, Choi HS, Frangioni JV. Image-guided surgery using invisible near-infrared light: fundamentals of clinical translation. Mol Imaging. 2010; 9:237–255. [PubMed: 20868625]
35. Marshall MV, Rasmussen JC, Tan I, et al. Near-infrared fluorescence imaging in humans with indocyanine green: a review and update. The Open Surgical Oncology Journal. 2010; 2:12–25.
36. Moody ED, Viskari PJ, Colyer CL. Non-covalent labeling of human serum albumin with indocyanine green: a study by capillary electrophoresis with diode laser-induced fluorescence detection. J Chromatogr B Biomed Sci Appl. 1999; 729:55–64. [PubMed: 10410927]
37. Ogawa M, Kosaka N, Choyke PL, et al. In vivo molecular imaging of cancer with a quenching near-infrared fluorescent probe using conjugates of monoclonal antibodies and indocyanine green. Cancer Res. 2009; 69:1268–1272. [PubMed: 19176373]
38. Landsman ML, Kwant G, Mook GA, et al. Light-absorbing properties, stability, and spectral stabilization of indocyanine green. J Appl Physiol. 1976; 40:575–583. [PubMed: 776922]
39. Alford R, Simpson HM, Duberman J, et al. Toxicity of organic fluorophores used in molecular imaging: literature review. Mol Imaging. 2009; 8:341–354. [PubMed: 20003892]
40. Speich R, Saesseli B, Hoffmann U, et al. Anaphylactoid reactions after indocyanine-green administration. Ann Intern Med. 1988; 109:345–346. [PubMed: 3395048]
41. Shimizu S, Kamiike W, Hatanaka N, et al. New method for measuring ICG Rmax with a clearance meter. World J Surg. 1995; 19:113–118. [PubMed: 7740796]
42. Ohnishi S, Lomnes SJ, Laurence RG, et al. Organic alternatives to quantum dots for intraoperative near-infrared fluorescent sentinel lymph node mapping. Mol Imaging. 2005; 4:172–181. [PubMed: 16194449]
43. Yoneya S, Saito T, Komatsu Y, et al. Binding properties of indocyanine green in human blood. Invest Ophthalmol Vis Sci. 1998; 39:1286–1290. [PubMed: 9620093]
44. philip R, Penzkofer A, Bäumler W, et al. Absorption and fluorescence spectroscopic investigation of indocyanine green. Journal of Photochemistry and Photobiology A: Chemistry. 1996:137–148.
45. Dreher MR, Liu W, Michelich CR, et al. Tumor vascular permeability, accumulation, and penetration of macromolecular drug carriers. J Natl Cancer Inst. 2006; 98:335–344. [PubMed: 16507830]
46. Nakajima M, Takeda M, Kobayashi M, et al. Nano-sized fluorescent particles as new tracers for sentinel node detection: experimental model for decision of appropriate size and wavelength. Cancer Sci. 2005; 96:353–356. [PubMed: 15958058]
47. Mariani G, Moresco L, Viale G, et al. Radioguided sentinel lymph node biopsy in breast cancer surgery. J Nucl Med. 2001; 42:1198–1215. [PubMed: 11483681]
48. Motomura K, Inaji H, Komoike Y, et al. Sentinel node biopsy guided by indocyanine green dye in breast cancer patients. Jpn J Clin Oncol. 1999; 29:604–607. [PubMed: 10721942]
49. Murawa D, Hirche C, Dresel S, et al. Authors' reply: Sentinel lymph node biopsy in breast cancer guided by indocyanine green fluorescence (Br J Surg 2009; 96: 1289–1294). Br J Surg. 2010; 97:455–456. [PubMed: 20140947]
50. van Akkooi AC, de Wilt JH, Verhoef C, et al. High positive sentinel node identification rate by EORTC melanoma group protocol. Prognostic indicators of metastatic patterns after sentinel node biopsy in melanoma. Eur J Cancer. 2006; 42:372–380. [PubMed: 16403622]
51. Clary BM, Brady MS, Lewis JJ, et al. Sentinel lymph node biopsy in the management of patients with primary cutaneous melanoma: review of a large single-institutional experience with an emphasis on recurrence. Ann Surg. 2001; 233:250–258. [PubMed: 11176132]
52. Bembenek A, Gretschel S, Schlag PM. Sentinel lymph node biopsy for gastrointestinal cancers. J Surg Oncol. 2007; 96:342–352. [PubMed: 17726666]

53. Ichikura T, Sugasawa H, Sakamoto N, et al. Limited gastrectomy with dissection of sentinel node stations for early gastric cancer with negative sentinel node biopsy. Ann Surg. 2009; 249:942–947. [PubMed: 19474686]
54. Ohdaira H, Nimura H, Mitsumori N, et al. Validity of modified gastrectomy combined with sentinel node navigation surgery for early gastric cancer. Gastric Cancer. 2007; 10:117–122. [PubMed: 17577622]
55. Kelder W, Nimura H, Takahashi N, et al. Sentinel node mapping with indocyanine green (ICG) and infrared ray detection in early gastric cancer: an accurate method that enables a limited lymphadenectomy. Eur J Surg Oncol. 2010; 36:552–558. [PubMed: 20452171]
56. Ishikawa K, Yasuda K, Shiromizu A, et al. Laparoscopic sentinel node navigation achieved by infrared ray electronic endoscopy system in patients with gastric cancer. Surg Endosc. 2007; 21:1131–1134. [PubMed: 17180275]
57. Ohdaira H, Nimura H, Takahashi N, et al. The possibility of performing a limited resection and a lymphadenectomy for proximal gastric carcinoma based on sentinel node navigation. Surg Today. 2009; 39:1026–1031. [PubMed: 19997796]
58. Markl B, Arnholdt HM, Jahnig H, et al. A new concept for the role of ex vivo sentinel lymph nodes in node-negative colorectal cancer. Ann Surg Oncol. 2010; 17:2647–2655. [PubMed: 20333553]
59. Buckle T, van Leeuwen AC, Chin PT, et al. A self-assembled multimodal complex for combined pre- and intraoperative imaging of the sentinel lymph node. Nanotechnology. 2010; 21 355101.
60. Hutteman M, Choi HS, Mieog JS, et al. Clinical Translation of Ex Vivo Sentinel Lymph Node Mapping for Colorectal Cancer Using Invisible Near-Infrared Fluorescence Light. Ann Surg Oncol. 2010
61. Mieog JS, Hutteman M, van der Vorst JR, et al. Image-guided tumor resection using real-time near-infrared fluorescence in a syngeneic rat model of primary breast cancer. Breast Cancer Res Treat. 2010
62. Pleijhuis RG, Graafland M, de VJ, et al. Obtaining adequate surgical margins in breast-conserving therapy for patients with early-stage breast cancer: current modalities and future directions. Ann Surg Oncol. 2009; 16:2717–2730. [PubMed: 19609829]
63. Ishizawa T, Bandai Y, Harada N, et al. Indocyanine green-fluorescent imaging of hepatocellular carcinoma during laparoscopic hepatectomy: An initial experience. Asian J Endosc Surg. 2010; 3:42–45.
64. Uchiyama K, Ueno M, Ozawa S, et al. Combined use of contrast-enhanced intraoperative ultrasonography and a fluorescence navigation system for identifying hepatic metastases. World J Surg. 2010; 34:2953–2959. [PubMed: 20734045]
65. Harada N, Ishizawa T, Muraoka A, et al. Fluorescence navigation hepatectomy by visualization of localized cholestasis from bile duct tumor infiltration. J Am Coll Surg. 2010; 210:e2–e6. [PubMed: 20510795]
66. Gotoh K, Yamada T, Ishikawa O, et al. A novel image-guided surgery of hepatocellular carcinoma by indocyanine green fluorescence imaging navigation. J Surg Oncol. 2009; 100:75–79. [PubMed: 19301311]
67. Miyoshi N, Ohue M, Noura S, et al. Surgical usefulness of indocyanine green as an alternative to India ink for endoscopic marking. Surg Endosc. 2009; 23:347–351. [PubMed: 18443867]
68. Fong Y, Cohen AM, Fortner JG, et al. Liver resection for colorectal metastases. J Clin Oncol. 1997; 15:938–946. [PubMed: 9060531]
69. Abdalla EK, Vauthey JN, Ellis LM, et al. Recurrence and outcomes following hepatic resection, radiofrequency ablation, and combined resection/ablation for colorectal liver metastases. Ann Surg. 2004; 239:818–825. [PubMed: 15166961]
70. Wei AC, Greig PD, Grant D, et al. Survival after hepatic resection for colorectal metastases: a 10-year experience. Ann Surg Oncol. 2006; 13:668–676. [PubMed: 16523369]
71. Pawlik TM, Scoggins CR, Zorzi D, et al. Effect of surgical margin status on survival and site of recurrence after hepatic resection for colorectal metastases. Ann Surg. 2005; 241:715–722. [PubMed: 15849507]

72. Karanjia ND, Lordan JT, Fawcett WJ, et al. Survival and recurrence after neo-adjuvant chemotherapy and liver resection for colorectal metastases: a ten year study. Eur J Surg Oncol. 2009; 35:838–843. [PubMed: 19010633]
73. Ishizawa T, Bandai Y, Ijichi M, et al. Fluorescent cholangiography illuminating the biliary tree during laparoscopic cholecystectomy. Br J Surg. 2010; 97:1369–1377. [PubMed: 20623766]
74. Aoki T, Murakami M, Yasuda D, et al. Intraoperative fluorescent imaging using indocyanine green for liver mapping and cholangiography. J Hepatobiliary Pancreat Sci. 2010; 17:590–594. [PubMed: 19844652]
75. Mitsuhashi N, Kimura F, Shimizu H, et al. Usefulness of intraoperative fluorescence imaging to evaluate local anatomy in hepatobiliary surgery. J Hepatobiliary Pancreat Surg. 2008; 15:508–514. [PubMed: 18836805]
76. Askin MP, Waye JD, Fiedler L, et al. Tattoo of colonic neoplasms in 113 patients with a new sterile carbon compound. Gastrointest Endosc. 2002; 56:339–342. [PubMed: 12196769]
77. Lee JG, Low AH, Leung JW. Randomized comparative study of indocyanine green and India ink for colonic tattooing: an animal survival study. J Clin Gastroenterol. 2000; 31:233–236. [PubMed: 11034004]
78. Maeda H, Wu J, Sawa T, et al. Tumor vascular permeability and the EPR effect in macromolecular therapeutics: a review. J Control Release. 2000; 65:271–284. [PubMed: 10699287]
79. Weinberg, AW. The Biology of Cancer. New York: Garland Science, Taylor & Francis Group, LLC; 2007.
80. Makino A, Kizaka-Kondoh S, Yamahara R, et al. Near-infrared fluorescence tumor imaging using nanocarrier composed of poly(L-lactic acid)-block-poly(sarcosine) amphiphilic polydepsipeptide. Biomaterials. 2009; 30:5156–5160. [PubMed: 19525007]
81. Intes X, Ripoll J, Chen Y, et al. In vivo continuous-wave optical breast imaging enhanced with Indocyanine Green. Med Phys. 2003; 30:1039–1047. [PubMed: 12852527]
82. Ntziachristos V, Yodh AG, Schnall M, et al. Concurrent MRI and diffuse optical tomography of breast after indocyanine green enhancement. Proc Natl Acad Sci U S A. 2000; 97:2767–2772. [PubMed: 10706610]
83. Alacam B, Yazici B, Intes X, et al. Pharmacokinetic-rate images of indocyanine green for breast tumors using near-infrared optical methods. Phys Med Biol. 2008; 53:837–859. [PubMed: 18263944]
84. Corlu A, Choe R, Durduran T, et al. Three-dimensional in vivo fluorescence diffuse optical tomography of breast cancer in humans. Opt Express. 2007; 15:6696–6716. [PubMed: 19546980]
85. Poellinger A, Burock S, Grosenick D, et al. Breast Cancer: Early- and Late-Fluorescence Near-Infrared Imaging with Indocyanine Green--A Preliminary Study. Radiology. 2010
86. Kimura T, Muguruma N, Ito S, et al. Infrared fluorescence endoscopy for the diagnosis of superficial gastric tumors. Gastrointest Endosc. 2007; 66:37–43. [PubMed: 17591472]
87. Iseki K, Tatsuta M, Iishi H, et al. Effectiveness of the near-infrared electronic endoscope for diagnosis of the depth of involvement of gastric cancers. Gastrointest Endosc. 2000; 52:755–762. [PubMed: 11115912]
88. Mataki N, Nagao S, Kawaguchi A. Clinical usefulness of a new infra-red videoendoscope system for diagnosis of early stage gastric cancer. Gastrointest Endosc. 2003; 57:336–342. [PubMed: 12612512]
89. ishihara R, Uedo N, Ishii H. Recent development and usefulness of infrared endoscopic system for diagnosis of gastric cancer. Dig Endosc. 2006; 18:45–48.
90. Reuthebuch O, Haussler A, Genoni M, et al. Novadaq SPY: intraoperative quality assessment in off-pump coronary artery bypass grafting. Chest. 2004; 125:418–424. [PubMed: 14769718]
91. Sekijima M, Tojimbara T, Sato S, et al. An intraoperative fluorescent imaging system in organ transplantation. Transplant Proc. 2004; 36:2188–2190. [PubMed: 15518796]
92. Kang Y, Lee J, Kwon K, et al. Dynamic fluorescence imaging of indocyanine green for reliable and sensitive diagnosis of peripheral vascular insufficiency. Microvasc Res. 2010; 80:552–555. [PubMed: 20637783]
93. Kang Y, Lee J, Kwon K, et al. Application of novel dynamic optical imaging for evaluation of peripheral tissue perfusion. Int J Cardiol. 2010; 145:e99–e101. [PubMed: 19230993]

94. Desai ND, Miwa S, Kodama D, et al. A randomized comparison of intraoperative indocyanine green angiography and transit-time flow measurement to detect technical errors in coronary bypass grafts. J Thorac Cardiovasc Surg. 2006; 132:585–594. [PubMed: 16935114]
95. Lee BT, Hutteman M, Gioux S, et al. The FLARE intraoperative near-infrared fluorescence imaging system: a first-in-human clinical trial in perforator flap breast reconstruction. Plast Reconstr Surg. 2010; 126:1472–1481. [PubMed: 21042103]
96. Pestana IA, Coan B, Erdmann D, et al. Early experience with fluorescent angiography in free-tissue transfer reconstruction. Plast Reconstr Surg. 2009; 123:1239–1244. [PubMed: 19337092]
97. Holm C, Mayr M, Hofter E, et al. Perfusion zones of the DIEP flap revisited: a clinical study. Plast Reconstr Surg. 2006; 117:37–43. [PubMed: 16404245]
98. Holm C, Mayr M, Hofter E, et al. Interindividual variability of the SIEA Angiosome: effects on operative strategies in breast reconstruction. Plast Reconstr Surg. 2008; 122:1612–1620. [PubMed: 19050513]
99. Betz CS, Zhorzel S, Schachenmayr H, et al. Endoscopic measurements of free-flap perfusion in the head and neck region using red-excited Indocyanine Green: preliminary results. J Plast Reconstr Aesthet Surg. 2009; 62:1602–1608. [PubMed: 19036663]
100. Newman MI, Samson MC. The application of laser-assisted indocyanine green fluorescent dye angiography in microsurgical breast reconstruction. J Reconstr Microsurg. 2009; 25:21–26. [PubMed: 18925547]
101. Komorowska-Timek E, Gurtner GC. Intraoperative perfusion mapping with laser-assisted indocyanine green imaging can predict and prevent complications in immediate breast reconstruction. Plast Reconstr Surg. 2010; 125:1065–1073. [PubMed: 20335859]
102. Yamaguchi S, De LF, Petit JY, et al. The "perfusion map" of the unipedicled TRAM flap to reduce postoperative partial necrosis. Ann Plast Surg. 2004; 53:205–209. [PubMed: 15480004]
103. Holm C, Dornseifer U, Sturtz G, et al. Sensitivity and specificity of ICG angiography in free flap reexploration. J Reconstr Microsurg. 2010; 26:311–316. [PubMed: 20183789]
104. Keereweer S, Kerrebijn JD, van Driel PB, et al. Optical Image-guided Surgery-Where Do We Stand? Mol Imaging Biol. 2010
105. Mieog JS, Vahrmeijer AL, Hutteman M, et al. Novel intraoperative near-infrared fluorescence camera system for optical image-guided cancer surgery. Mol Imaging. 2010; 9:223–231. [PubMed: 20643025]
106. Hutteman M, Mieog JS, van der Vorst JR, et al. Intraoperative near-infrared fluorescence imaging of colorectal metastases targeting integrin avb3 expression in a syngeneic rat model. Eur J Surg Oncol. 2010 Accepted for publication.
107. Adams KE, Ke S, Kwon S, et al. Comparison of visible and near-infrared wavelength-excitable fluorescent dyes for molecular imaging of cancer. J Biomed Opt. 2007; 12 024017.
108. Weissleder R, Tung CH, Mahmood U, et al. In vivo imaging of tumors with protease-activated near-infrared fluorescent probes. Nat Biotechnol. 1999; 17:375–378. [PubMed: 10207887]
109. Kuil J, Velders AH, van Leeuwen FW. Multimodal tumor-targeting peptides functionalized with both a radio- and a fluorescent label. Bioconjug Chem. 2010; 21:1709–1719. [PubMed: 20812730]
110. Marshall MV, Draney D, Sevick-Muraca EM, et al. Single-Dose Intravenous Toxicity Study of IRDye 800CW in Sprague-Dawley Rats. Mol Imaging Biol. 2010
111. van der Pas MH, van Dongen GA, Cailler F, et al. Sentinel node procedure of the sigmoid using indocyanine green: feasibility study in a goat model. Surg Endosc. 2010; 24:2182–2187. [PubMed: 20177933]
112. Gioux S, Mazhar A, Cuccia DJ, et al. Three-dimensional surface profile intensity correction for spatially modulated imaging. J Biomed Opt. 2009; 14 034045.
113. Kumar AT, Raymond SB, Bacskai BJ, et al. Comparison of frequency-domain and time-domain fluorescence lifetime tomography. Opt Lett. 2008; 33:470–472. [PubMed: 18311295]
114. Themelis G, Yoo JS, Soh KS, et al. Real-time intraoperative fluorescence imaging system using light-absorption correction. J Biomed Opt. 2009; 14 064012.

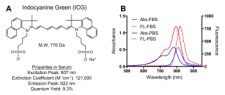

Fig. 1.

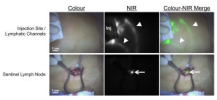

Fig. 2.

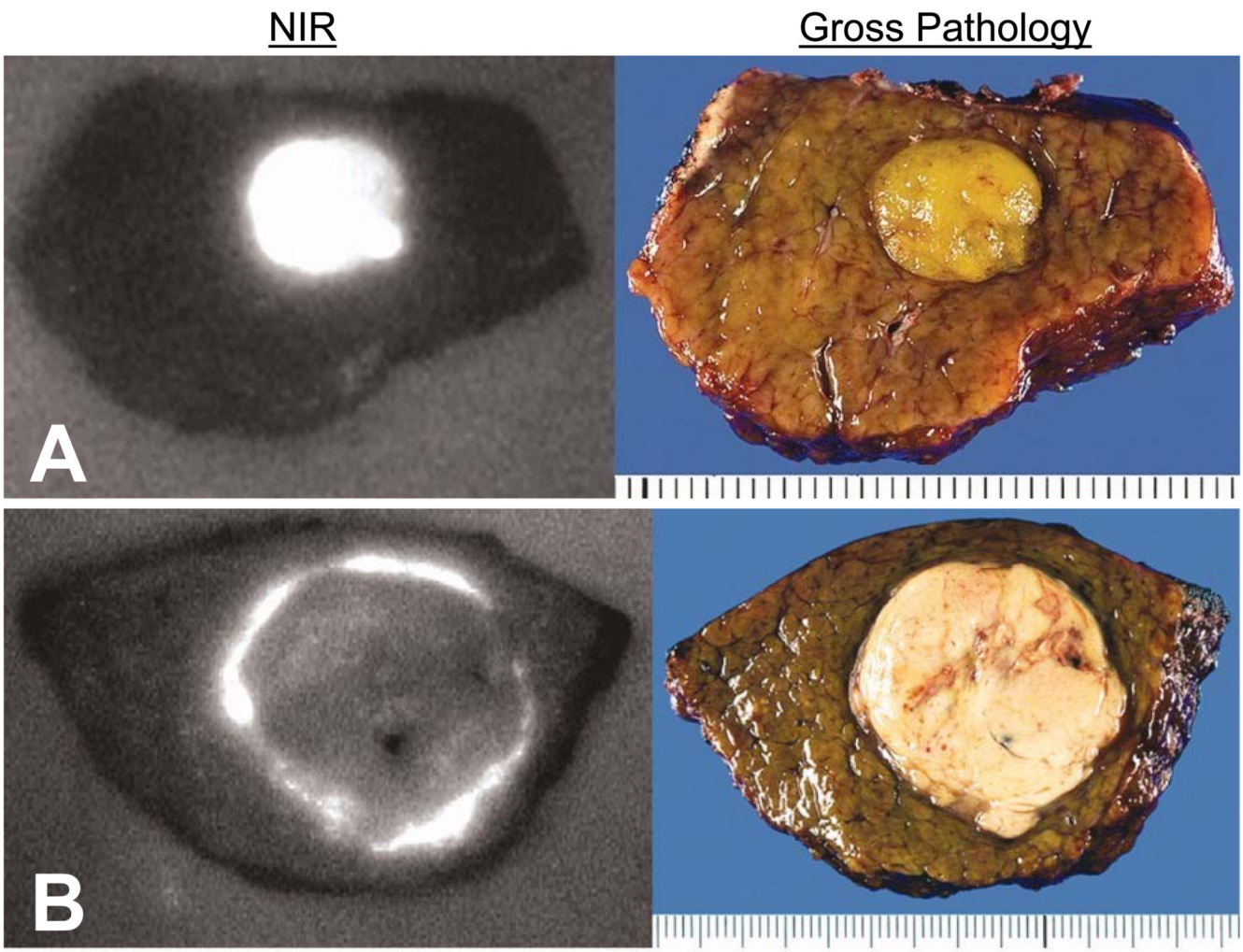

Fig. 3.

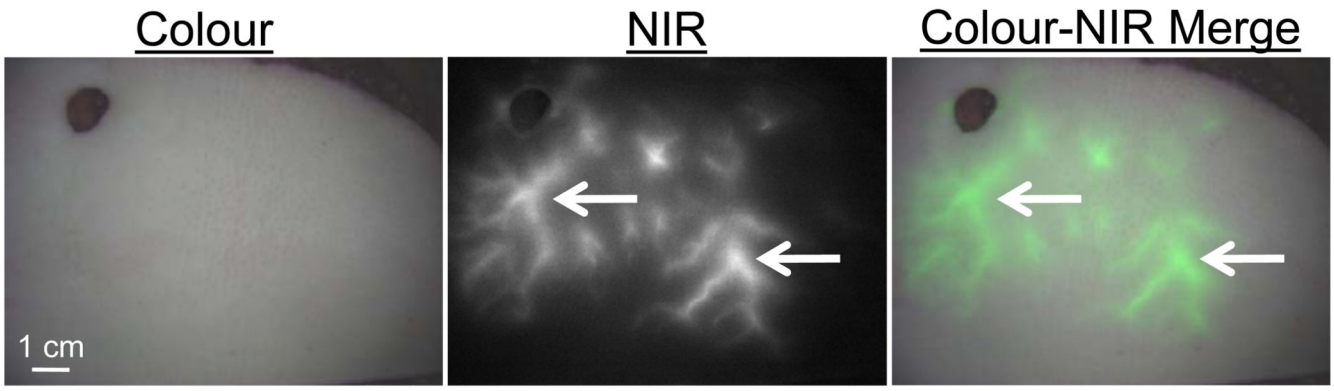

Fig. 4.

Table I

Clinically available imaging systems.

Imaging system	Excitation source	Working distance	Field of view	White light illumination of surgical field	NIR-colour overlay
PDE	LED 805 nm, power NS	15–25 cm	NS	No	No
SPY	Laser 806 nm, 2.0 W	30 cm	56 cm^2	No	No
Fluobeam	Laser 780 nm, 10mW/cm^2	22 cm	80 cm^2	Yes	No
HyperEye	LED 760 nm, power NS	30–50 cm	78.5 cm^2	Yes	Yes
FLARE	LED 745–779 nm, 14 mW/cm^2	45 cm	3.7 cm^2–169.5 cm^2	Yes	Yes
Mini-FLARE	LED 760 nm, 8.6 mW/cm^2	30 cm	100 cm^2	Yes	Yes
FDPM imager	Laser Diode 785 nm ± 10 nm, <1.9 mW/cm^2	<76.2 cm	Max 900 cm^2	No	No
Munich / SurgOptix prototype camera system	Laser 750 nm, 300 mW	21 cm	1,5 cm^2–107 cm^2	Yes	Yes

PDE, Photodynamic Eye; LED, Light emitting diode; NS, not specified; FLARE, Fluorescence-Assisted Resection and Exploration; FDPM, Frequency Domain Photon Migration

Table II

Clinical trials using ICG as a near-infrared fluorescent lymphatic tracer for SLN procedures.

Study	Year	No pat.	Tumor stage	Imaging system	Dose of ICG	Site of injection	Other used SLN tracer	IR (%)	FNR	Avg no SLNs
Breast Cancer										
Kitai[13]	2005	18	T1-2, cN0	PDE	5.0 ml, 6.4 mM	subareolar	none	94	NA	2.8
Ogasawara[19]	2008	37	Tis-T4	PDE	5.0 ml, 6.4 mM	s.c. subareolar and peritumoral	BD or BD + RT	NA	NA	NA
Sevick-Muraca[16]	2008	24	< 3 cm, cN0	FDPM imager	0.1–3.0 ml, 0.31–100 μg†	s.c. periareolar and/or i.c. and deep peritumoral	RT	87.5§	NA	1.7§
Tagaya[18]	2008	25	< 3 cm	PDE	1.0 ml, 6.4 mM	s.c. periareolar	BD	100	NA	5.4
Troyan[3]	2009	6	T1	FLARE	1.6 ml, 0.01 mM ICG:HSA	deep and s.c. peritumoral	RT	100	NA	1.5
Murawa[12]	2009	30	< 3 cm, cN0	IC-view	1.0–3.0 ml, 6.4 mM	i.c. periareolar	None or RT	97	2/21	1.75
Hirche[14]	2010	43	< 3 cm, cN0	IC-view	11 mg†	subareolar	BD	97.7	1/18	2.0
Hojo[15]	2010	141	Tis-T2, cN0	PDE	2.0 ml†	i.c. peritumoral and subareolar	BD or RT	99.3	NA	3.8
Tagaya[20]	2010	150	< 3 cm, cN0	PDE	0.75 ml, 3.2 mM	s.c. periareolar	BD	98.7	NA	3.7
Tagaya[21]	2010	50	< 2 cm, cN0	PDE	1.0 ml, 1.6 mM	s.c. periareolar	BD	100	NA	3.7
Mieog[17]	2011	24	Tis-T2, cN0	Mini-FLARE	1.6 ml, 0.05 – 1 mM	i.c. periareolar or s.c. peritumoral	BD + RT	100	NA	1.45
Skin Cancer										
Fujiwara[22]	2008	10	MM, SCC, T1-4, cN0-3	PDE	0.6–0.8 ml, 6.4 mM	peritumoral	None or BD	100	NA	NA
Tanaka[24]	2009	6	MM, EPD, SCC	PDE	1.0 ml, 6.4–10.2 mM	peritumoral	RT	100	NA	NA
Tsujino[25]	2009	2	EPD, SCC	PDE	1.0 ml, 6.4 mM	intra- or peritumoral	RT	100	NA	NA
Mizukami[23]	2010	24	MM, EPD, SCC, EPC	PDE	0.6–2.0 ml, 6.4 mM	peritumoral	none	95.8	NA	NA
Gastro-Intestinal Cancer										
Kusano[26]	2008	22	Gastric T1-3,	PDE	2.0 ml, 6.4 mM	s.s. intraoperative	none	90.9	6/10	3.6
		26	Colorectal T1-3					88.5	4/6	2.6
Miyashiro[27]	2008	3	Gastric T1	PDE	2.0–4.0 ml†	intra- or 1 day	none	100	NA	3.0

Study	Year	No pat.	Tumor stage	Imaging system	Dose of ICG	Site of injection	Other used SLN tracer	IR (%)	FNR	Avg no SLNs
						preoperative				
Tajima[28]	2009	56	Gastric pT1-3	PDE	2.0 ml, 6.4 mM	s.m. 1–3 days preoperative or s.s. intraoperative	none	96.4	6/17	7.2
Noura[7]	2009	25	Rectal T1-3	PDE	1.0 ml, 6.4 mM	s.m. before laparotomy	none	92	0/3	2.1
Tajima[29]	2010	77	Gastric T1-3	PDE	2.0 ml, 6.4 mM	s.m. 1–3 days preoperative or s.s. intraoperative	none	94.8	4/17	7.5
Other Cancer										
Crane[4]	2010	10	Stage IA1, IB1, IIA cervical cancer	Munich prototype	1.0 ml, 0.64 mM	intraoperative in four quadrants of the cervix	BD	60 in vivo	0/1	1.5
Crane[8]	2010	10	Stage T1/2 vulvar cancer	Munich prototype	1.0 ml, 0.64 mM	peritumoral	BD + RT	100	NA	2.6
Bredell[9]	2010	8	Oropharyngeal cancer	PDE	1.0 ml, 12.9 mM	peritumoral	none	100	NA	3.0
Yamashita[10]	2010	31	Stage I non-small-cell lung cancer	NS	2.0 ml, 6,4 mM	peritumoral	none	80.7	NA	1.3
Hirche[11]	2010	12	Anal squamous-cell cancer, cN0	IC-View	5.0 ml, 6.4 mM	peritumoral subdermal	BD + RT	83.3	NA	1.6

IR, identification rate; FNR, false-negative rate; NA, not available; s.c., subcutaneous; BD, blue dye; RT, radiotracer; i.c., intracutaneous; ICG:HSA, indocyanine green adsorbed to human serum albumin; MM, malignant melanoma; SCC, squamous cell carcinoma; EPD, extramammary Paget's disease; EPC, eccrine porocarcinoma; s.s., subserosal; s.m., submucosal; NS, not specified.

[†] Concentration not available

[§] Only in those patients receiving > 10 μg ICG (N = 7)